

See discussions, stats, and author profiles for this publication at: <https://www.researchgate.net/publication/263939712>

# Osmolytic Co-Solute Perturbing the Surface Enhancement of Halide Ions

ARTICLE *in* JOURNAL OF PHYSICAL CHEMISTRY LETTERS · AUGUST 2013

Impact Factor: 7.46 · DOI: 10.1021/jz4014695

---

CITATIONS

3

---

READS

6

2 AUTHORS, INCLUDING:



Xiaohu Li

Sandia National Laboratories

15 PUBLICATIONS 138 CITATIONS

SEE PROFILE

## Osmolytic Co-Solute Perturbing the Surface Enhancement of Halide Ions

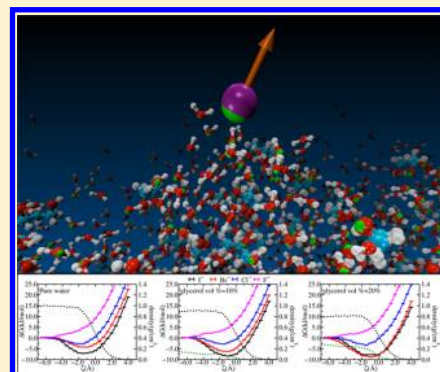
Xiaohu Li<sup>‡</sup> and George C. Schatz\*

Department of Chemistry, Northwestern University, 2145 Sheridan Road, Evanston, Illinois 60208-3113, United States

## S Supporting Information

**ABSTRACT:** We have investigated the variation in the surface binding free energy with the choice of halide ion,  $F^-$ ,  $Cl^-$ ,  $Br^-$ , and  $I^-$ , in water–glycerol binary mixtures with varying glycerol concentrations using umbrella sampling with a polarizable force field. We have found that halide surface adsorption is significantly perturbed by glycerol. At no or low glycerol concentration, the surface preference follows the Hofmeister series ( $I^- > Br^- > Cl^- > F^-$ ). However, at the highest concentration,  $Br^-$  is preferentially stabilized. Decomposition of the free energy indicates that the halide surface adsorption is dominated by enthalpy and, specifically, by the solvent–solvent polarization interaction. The differences in this interaction between the chaotropic halides are reduced by glycerol addition, which is in line with a recent measurement of the solvent excess enthalpy for the same systems studied here. Moreover, our calculations indicate that the effect of an osmolyte (glycerol) on surface ion concentrations parallels the known effect of osmolytes on protein folding.

**SECTION:** Surfaces, Interfaces, Porous Materials, and Catalysis



Ion adsorption at aqueous interfaces has been one of the most intensively debated subjects in chemistry for the past century.<sup>1–6</sup> A commonly held theory attributes specific ion adsorption to the abilities of ions to enhance/break the hydrogen bonding network of water. However, recent studies have shown that an array of factors can affect aqueous ion surface concentrations, including ion polarizability, van der Waals interaction, and direct interaction between ions and interfaces.<sup>2</sup> The ordering of the abilities of ions to cause folding or denaturation of proteins in solution, which is expressed in terms of the widely known Hofmeister series, is closely related to this surface adsorption behavior.

Protective osmolytes, such as polyols, have been found to stabilize the structures of proteins,<sup>7–9</sup> to significantly reduce the cooling rate of water for glass formability,<sup>10</sup> to protect cells from freezing in aqueous solutions,<sup>11</sup> and even to reverse the misfolding of protein in genetic lesions.<sup>12</sup> Both experimental and theoretical studies have pointed out that the osmolyte stabilization effect is enthalpic in nature.<sup>7,9</sup> However, studies of the effects of osmolytes on aqueous ions are scarce, despite the fact that ions and osmolytes coexist in living cells.<sup>8</sup> A natural question to ask is, Are the stabilizing/destabilizing effects of osmolytes and ions on the folding of proteins, or on the surface concentration of ions, additive?

In this study, we have utilized molecular dynamics (MD) simulations with a state-of-the-art polarizable force field as implemented in the high-performance MD code NAMD<sup>13</sup> to probe this question.<sup>14,15</sup> The polarizability in this Drude oscillator model is accounted for by attaching an auxiliary particle to the parent atom via a spring. This implementation of polarizability maintains the simple particle–particle Coulomb

electrostatic interaction employed in nonpolarizable force fields. Furthermore, an extended Lagrangian scheme with a dual-Langevin thermostat applied to the Drude nucleus pairs was also developed to circumvent the prohibitive self-consistent field (SCF) procedure. This enables the efficient generation of classical trajectories that are near the SCF limit.

The potential-of-mean-force (PMF) for surface adsorption of halide ions ( $F^-$ ,  $Cl^-$ ,  $Br^-$ ,  $I^-$ ) has been determined for three different water/glycerol solutions using MD calculations and a force field that includes a Drude oscillator model for polarization effects. The SWM4-NDP potential,<sup>16,17</sup> which is known to reproduce various properties of water including structure, self-diffusion, and surface tension, was adopted to describe the water portion of the simulation. A nonpolarizable CHARMM force field for polyols is available; however, it produced noticeable deviations from experimental values of the density and diffusion coefficient for glycerol.<sup>18</sup> There are currently few choices of force field that include polarization for glycerol, that is, such as those implemented in AMOEBA.<sup>19</sup> However, a detailed validation of the properties of the glycerol–water mixture is lacking. In the present study, we have transferred the parameters of the Drude particle force field, as parametrized for the primary and secondary alcohol series,<sup>20</sup> to those for glycerol. No effort has been made to reparametrize those parameters. As it turns out, the results are remarkably good for various properties of water–glycerol mixtures (see the Supporting Information (SI)). The well-

Received: July 15, 2013

Accepted: August 11, 2013

Published: August 12, 2013



tested Drude force field parameters for monovalent and divalent ions<sup>21</sup> were used for the halide ions. We were able to include as many as 1000 polarizable waters in this study due to the highly parallel nature of the Drude model in NAMD. To our knowledge, the studies presented in this letter represent the first investigation of surface adsorption of halide ions in the water/polyol mixture solutions with many-body polarization effects accounted for.

Pure glycerol is an extremely viscous liquid. As seen in the SI, as the percentage of glycerol grows in the water–glycerol mixture, the diffusion coefficients for both water and glycerol decrease. Experiment has shown that solutions with a glycerol volume percentage higher than 40% become rather viscous.<sup>7</sup> Thus, to avoid convergence problems in MD simulations, mixtures with 0, 10, and 20% glycerol (mass %: 0, 12.5, and 24.1%; mole fraction: 0, 0.027, 0.058) by volume are investigated.

A snapshot of a halide ion being pulled out of the surface of a water–glycerol mixture is shown in Figure 1. The PMFs for

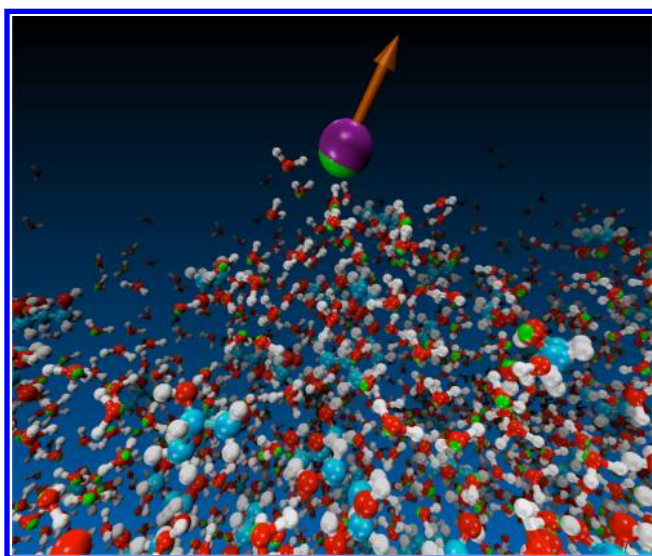


**Figure 1.** A schematic representation of a halide ion being pulled out of a water–glycerol mixture surface extracted from simulation. In this picture, spheres with purple, light cyan, red, and white represent the halide ion, carbons, oxygens, and hydrogens, respectively. The green spheres are Drude particles. The orange arrow is a cartoon representation of the induced dipole moment of the halide–Drude pair.

halide ion solvation along the surface normal in the three different mixtures are presented in Figure 2. We first notice that

the number density of glycerol (green dotted lines in Figure 2) is negligible compared to the water density (black dotted line) near the Gibbs dividing surface (GDS) at  $\zeta = 0$  Å (see the SI for the definition of the GDS). To partially understand this difference, we have resolved the water–solvent (including water–water and water–glycerol) and glycerol–solvent interactions (per water or glycerol) according to their positions along the surface normal (see the SI for details). The water–solvent energy while water is located at the surface is 7.45 and 7.90 kJ/mol higher than that in the bulk for the 10 and 20% mixtures respectively. In comparison, the glycerol–solvent interaction for glycerol at the surface is 12.18 and 12.69 kJ/mol higher relative to the bulk. Thus, compared to a water molecule, a glycerol is energetically less favorable at the surface. We caution that the entropy effects are not accounted for in these energy calculations; thus, a full picture would necessitate a PMF calculation similar to those for the halide ions. This will be presented in future studies. This energy difference between glycerol and water is reminiscent of what is seen at the water/protein interface in aqueous glycerol solution.<sup>7,9</sup>

We notice from Figure 2 that the surface adsorption preference of the halides in pure water follows the Hofmeister series,<sup>1,2</sup> that is, the surface adsorption energy, defined as the difference in free energy between the minimum near the GDS and the plateau in the bulk region, satisfies  $\Delta G_F < \Delta G_{Cl} < \Delta G_{Br} < \Delta G_I$ . These results are in good agreement with previous studies, including results using a cluster model for water with a different version of the Drude polarizable force field (positive charges were assigned to the Drude particles, as opposed to the negative charges used here).<sup>3</sup>

Upon the addition of glycerol, the surface preferences for all halides except fluoride increase in general (see Table 1). If

**Table 1.** Depth of PMF Minima for Halide Ions<sup>a</sup>

	water	glycerol 10%	glycerol 20%
F <sup>−</sup>	n/a	n/a	n/a
Cl <sup>−</sup>	−2.72(0.06)	−2.84(0.05)	−3.39(0.05)
Br <sup>−</sup>	−4.25(0.06)	−6.30(0.05)	−8.72(0.05)
I <sup>−</sup>	−7.11(0.06)	−8.38(0.05)	−7.78(0.05)

<sup>a</sup>The units are kJ/mol, and error bars are given in parentheses.

there is a direct correspondence between ion–surface adsorption and the ability of an ion to cause protein folding or unfolding, then these results suggest that a kosmotrope (which causes the protein to fold) such as F<sup>−</sup> is not significantly affected by glycerol, while chaotropes (causing the denaturation of protein) such as Cl<sup>−</sup>, Br<sup>−</sup>, and I<sup>−</sup> are enhanced by the

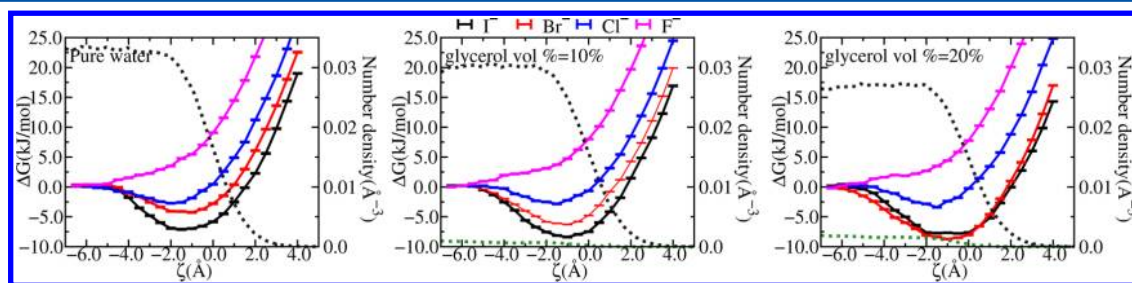


**Figure 2.** PMF for solvation along the surface normal for three different water–glycerol mixture solutions for F<sup>−</sup>, Cl<sup>−</sup>, Br<sup>−</sup>, and I<sup>−</sup>. Black and green dotted lines represent reduced water and glycerol densities, respectively. The GDS has been shifted to  $\zeta = 0$  Å in all graphs. In all graphs, error bars are shown and are  $\sim 0.07$  kJ/mol. The error estimation is obtained using a bootstrap analysis.<sup>22</sup>



addition of glycerol. Furthermore, this increase in surface adsorption depends on the glycerol concentration, that is, while  $\text{Cl}^-$  and  $\text{Br}^-$  increase with glycerol concentration, with  $\text{Br}^-$  rising much more significantly,  $\text{I}^-$  seems to saturate after 10% glycerol concentration. This glycerol concentration dependence causes alteration of the order of interfacial preference of these chaotropes such that the surface adsorption energy of bromide is slightly higher than that of iodide at 20% glycerol by volume. In other words,  $\text{Br}^-$  is preferentially stabilized at the surface relative to  $\text{I}^-$  as glycerol increases. We note that a similar glycerol concentration dependence was observed when the optimum rate of cooling for the survival of cells was measured.<sup>11</sup>

To investigate the molecular mechanism for the change in ordering of the surface preference, we first decompose the free energy into enthalpic and entropic contributions. We have ignored the pressure–volume work in this analysis because it is negligible under ambient conditions. The results are presented in Figure 3. This shows that except for fluoride, the three ions

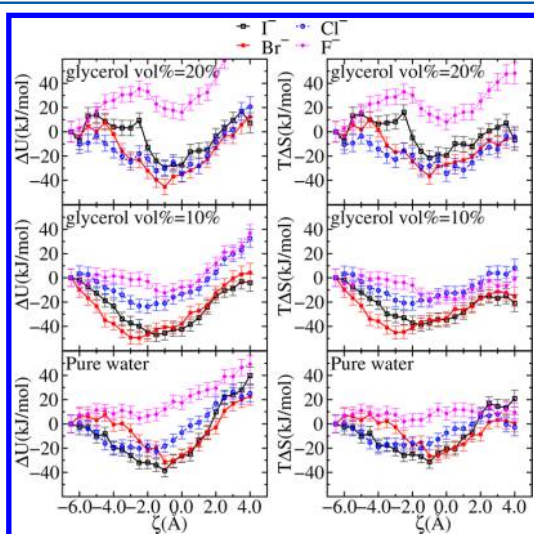


**Figure 3.** Enthalpic ( $\Delta U$ ) and entropic ( $T\Delta S$ ) contributions to the PMF of halide ions in all three liquid compositions. Both enthalpy and entropy terms are shifted using values for the bulk ( $\zeta = -6.5$  Å). Except for fluoride, all of the other three ions display minima near the GDS in both enthalpic and entropic contributions. However, the depths of the minima for the three ions change order upon the addition of glycerol, in accordance with that of PMF. Error bars were estimated using a bootstrap analysis.<sup>22</sup>

show narrow minima around the GDS for both enthalpic and entropic terms regardless of the glycerol concentration. Although whether the contribution of enthalpy is canceled by the entropic term is a subject of debate,<sup>24–27</sup> our calculation clearly shows that the enthalpy term dominates over entropy, thus giving rise to the surface adsorption minima in the PMF for these three ions. A similar phenomenon has been found for halide ions in water (either cluster or slab)<sup>3,27</sup> and thiocyanate in liquid water.<sup>23</sup> However, as glycerol is added into the solution, the landscape as well as the depth of the minima for the halide ions is significantly altered. Thus, the order of the depth of the minima in both enthalpy and entropy in pure water is  $\text{I}^- > \text{Br}^- > \text{Cl}^- > \text{F}^-$ , while this order changes to  $\text{Br}^- > \text{I}^- > \text{Cl}^- > \text{F}^-$  at 10% glycerol and eventually to  $\text{Br}^- > \text{I}^- \approx \text{Cl}^- > \text{F}^-$  in the enthalpy results and  $\text{Br}^- \approx \text{Cl}^- > \text{I}^- > \text{F}^-$  in the entropy results for 20% glycerol. Specifically, the minima in

both the enthalpic and entropic terms for  $\text{Br}^-$  and  $\text{I}^-$  switch order as glycerol is added, that is, at the highest glycerol concentration, the minimum in enthalpy for  $\text{Br}^-$  is about 20 kJ/mol lower than that for  $\text{I}^-$ . This, of course, is in accordance with the change of order in surface preference for  $\text{Br}^-$  and  $\text{I}^-$  as seen in Figure 2. Hence, the enthalpy is the dominant force that drives the switch in order of the surface adsorption for  $\text{Br}^-$  and  $\text{I}^-$ .

To better understand the molecular mechanism of this enthalpy-driven phenomenon, we further divide the enthalpy term into solvent–solvent and solvent–ion terms. We note that this division is not theoretically rigorous for a polarizable force field due to its many-body nature. In our simulations, because of the low concentration of halide ions ( $\sim 0.06$  M, realized through the large number of water and glycerol molecules used), we found that only solvent molecules that are locally coordinated to the halide ion are significantly polarized by its field. From the left column of Figure 4a, it is clear that at no or low glycerol concentration, the depth of the solvent–solvent interaction roughly follows the original Hofmeister series. However, at the highest glycerol concentration, the depth of the minima for all three chaotropes is the same within the error bars, although there is a trend for the ordering to be changed to  $\text{Br}^- \approx \text{Cl}^- > \text{I}^- > \text{F}^-$ , similar to the order in the enthalpy term. Westh et al.<sup>28</sup> have measured the glycerol–glycerol enthalpic interaction in a ternary glycerol–halide–water system using a second-order differential form of the excess enthalpy. This interaction follows the original Hofmeister series at infinitesimal glycerol mole fraction. However, at  $x_{\text{Gly}} = 0.1$ , these differences become negligible. This is in agreement with our observation that the depths of the minima in the solvent–solvent interactions for all three chaotropes are similar at 20% ( $x_{\text{Gly}} = 0.058$ ). Although it is difficult for us to directly compare the second-order differential term due to large statistical fluctuations presumably caused by the limited number of glycerols used in our simulations, the agreement between our results and those in ref 28 is rather encouraging.

In the point-dipole approximation, the polarization energy is roughly the negative of the induction energy (see the SI) that comes from induced dipoles in a static field.<sup>29</sup> Hence, we have used  $U_{\text{pol}} \approx -U_{\text{ind}}$  to estimate how electronic polarization plays a role in the solvent–solvent interaction. The results are presented in the right column in Figure 4a. It is clear that the induction energy from polarization is dominant in determining the landscape of the solvent–solvent interaction because the depth of the minima (maxima in the polarization energy because  $U_{\text{pol}} \approx -U_{\text{ind}}$ ) is comparable to the total solvent–solvent term. In addition, as glycerol is added, the depth of the minima of the induction energy term ( $-\Delta U_{\text{sol-pol}}$ ) of the chaotropes changes order from the original Hofmeister series at no or low glycerol concentration to  $\text{Cl}^- > \text{Br}^- > \text{I}^- > \text{F}^-$  at 20%, suggesting that polarization is largely responsible for the enthalpy-driven reordering of the halide surface preferences.

In Figure 4b, the solvent–ion interaction landscape for the halide ions is displayed. Unlike the total enthalpy and solvent–solvent interaction terms, the solvent–ion term continues to rise as the ions are pulled toward the surface. Furthermore, although the addition of glycerol does bring the energy landscapes of the ion–solvent interaction closer for all four halides, this dependence is relatively insensitive to the addition of glycerol as compared to the solvent–solvent term. We have also provided the energy landscape of the ion polarization in the right column of Figure 4b. It is clear that this term does not

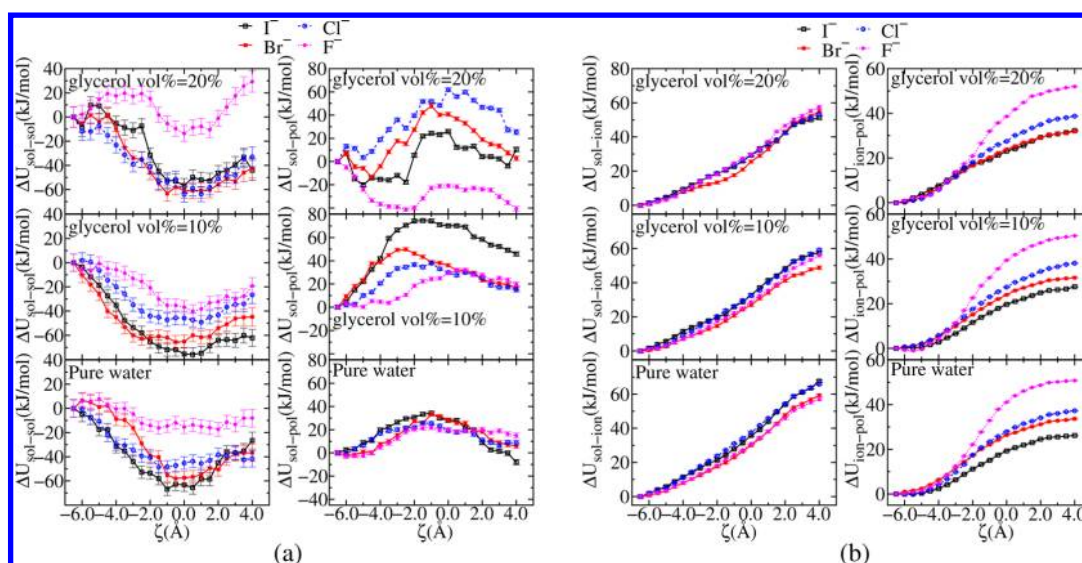


**Figure 4.** (Left) Solvent–solvent interaction ( $\Delta U_{\text{sol-sol}}$ ) and polarization energy of the solvent ( $\Delta U_{\text{sol-pol}}$ ). (Right) Solvent–ion interaction ( $\Delta U_{\text{sol-ion}}$ ) and polarization energy of the halide ions ( $\Delta U_{\text{ion-pol}}$ ). All curves are shifted using values at the bulk ( $\zeta = -6.5$  Å). Error bars were estimated using a bootstrap analysis.<sup>22</sup>

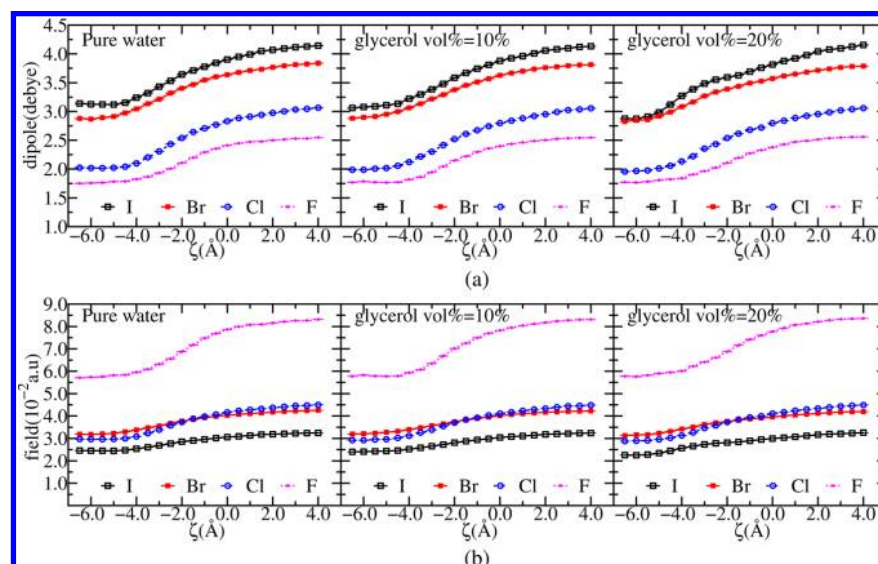


**Figure 5.** (a) Profiles of dipole moments of the halide ions as they are pulled through the liquid interfaces. The origin for calculating the dipole is located at the parent atom of the halide atom–Drude particle pair. (b) The electric field  $E_{\text{anion}}$  on the halide atom as a function of position along the surface normal.

change significantly with glycerol concentration, although there is a slight increase for  $\text{I}^-$ . However, compared to the polarization energy from the solvent, ion polarization plays a secondary role in determining the final PMF for ion adsorption.

It has been argued that it is the induced dipole of halide ions at the interface in the polarizable models that enhances the ion induction energy.<sup>30</sup> Indeed, our calculations show that as the ions are pulled out of the liquid, the induced dipole moment increases (see Figure 5a), with the induced dipole following the order of their polarizabilities. However, the stronger binding of  $\text{F}^-$  to solvent, characterized by its large hydration energy, also causes  $\text{F}^-$  to experience a larger electric field magnitude from the solvent. Thus, the final induction energy  $(-1/2)\sum_i \mu_i \cdot E_i^{(0)}$  of the halide ion (see the SI) follows the order (see the right column of Figure 4b)  $\text{F}^- > \text{Cl}^- > \text{Br}^- > \text{I}^-$ . This suggests that the surface adsorption energies of the halide ions are not

determined by their polarizability. Rather, our results show that they are dominated by solvent polarization and secondarily affected by the ion polarization energy. This applies both to pure water, where it leads to the usual Hofmeister results, and to the water–glycerol mixtures, where the Hofmeister trends are partially reversed.

To summarize, we have presented results pertaining to ion adsorption at the air/liquid interfaces for water–glycerol mixtures with various glycerol concentrations. It is found that halide ion surface adsorption is significantly affected by the addition of glycerol. At no or low glycerol concentration, the surface preference follows the original Hofmeister series. However, at the highest glycerol concentration,  $\text{Br}^-$  is preferentially stabilized at the surface. Decomposition of the free energy into enthalpic and entropic terms indicates that halide surface adsorption is dominated by enthalpy and,



specifically, by solvent–solvent interaction. Furthermore, the energy landscape of solvent–solvent interaction as ions are pulled through the interface is dominated by many-body polarization of the solvent. The change in the polarization landscape of both the solvent and ions as the glycerol concentration changes drives this effect. This study sheds light on the interplay between ions and osmolytes on aqueous interfaces, showing that osmolyte effects on the role of halides in protein denaturation also show up in halide surface concentrations. We hope that this can initiate further studies of the stabilizing effects of osmolytes on protein folding.

## ■ ASSOCIATED CONTENT

### ■ Supporting Information

Computational details including parameters used in MD, validation of the Drude polarizable force field for the water–glycerol mixtures, details about the PMF calculation, resolution of water–solvent and glycerol–solvent energies in the interfacial and bulk regions, and the energy expression of the Drude polarizable force field. This material is available free of charge via the Internet at <http://pubs.acs.org>.

## ■ AUTHOR INFORMATION

### Corresponding Author

\*E-mail: [schatz@chem.northwestern.edu](mailto:schatz@chem.northwestern.edu).

### Present Address

\*X.L.: Combustion Research Facility, Sandia National Laboratories, Livermore, CA 94550.

### Notes

The authors declare no competing financial interest.

## ■ ACKNOWLEDGMENTS

This work has been supported by NSF Grant CHE-1147335.

## ■ REFERENCES

- (1) Zhang, Y.; Cremer, P. S. Chemistry of Hofmeister Anions and Osmolytes. *Annu. Rev. Phys. Chem.* **2010**, *61*, 63–83.
- (2) Lo Nostro, P.; Ninham, B. W. Hofmeister Phenomena: An Update on Ion Specificity in Biology. *Chem. Rev.* **2012**, *112*, 2286–2322.
- (3) Caleman, C.; Hubb, J. S.; van Maaren, P. J.; van der Spoel, D. Atomistic Simulation of Ion Solvation in Water Explains Surface Preference of Halides. *Proc. Natl. Acad. Sci. U.S.A.* **2011**, *108*, 6838–6842.
- (4) Chang, T.-M.; Dang, L. X. Recent Advances in Molecular Simulations of Ion Solvation at Liquid Interfaces. *Chem. Rev.* **2006**, *106*, 1305–1322.
- (5) Jungwirth, P.; Tobias, D. J. Specific Ion Effects at the Air/Water Interface. *Chem. Rev.* **2006**, *106*, 1259–1281.
- (6) Petersen, P. B.; Saykally, R. J. On the Nature of Ions at the Liquid Water Surface. *Annu. Rev. Phys. Chem.* **2006**, *57*, 333–364.
- (7) Gekko, K.; Timasheff, S. N. Mechanism of Protein Stabilization by Glycerol: Preferential Hydration in Glycerol–Water Mixtures. *Biochemistry* **1981**, *20*, 4667–4676.
- (8) Yancey, P. H.; Clark, M. E.; Hand, S. C.; Bowlus, R. D.; Somero, G. N. Living with Water Stress: Evolution of Osmolyte Systems. *Science* **1982**, *217*, 1214–1222.
- (9) Gilman-Politi, R.; Harries, D. Unraveling the Molecular Mechanism of Enthalpy Driven Peptide Folding by Polyol Osmolytes. *J. Chem. Theory Comput.* **2011**, *7*, 3816–3828.
- (10) Warkentin, M.; Sethna, J. P.; Thorne, R. E. Critical Droplet Theory Explains the Glass Formability of Aqueous Solutions. *Phys. Rev. Lett.* **2013**, *110*, 015703.
- (11) Mazur, P. Cryobiology: The Freezing of Biological Systems. *Science* **1970**, *168*, 939–949.

- (12) Sato, S.; Ward, C. L.; Krouse, M. E.; Wine, J. J.; Kopito, R. R. Glycerol Reverses the Misfolding Phenotype of the Most Common Cystic Fibrosis Mutation. *J. Biol. Chem.* **1996**, *271*, 635–638.
- (13) Phillips, J. C.; Braun, R.; Wang, W.; Gumbart, J.; Tajkhorshid, E.; Villa, E.; Chipot, C.; Skeel, R. D.; Kalé, L.; Schulten, K. Scalable Molecular Dynamics with NAMD. *J. Comput. Chem.* **2005**, *26*, 1781–1802.
- (14) Lamoureux, G.; Roux, B. Modeling Induced Polarization with Classical Drude Oscillators: Theory and Molecular Dynamics Simulation Algorithm. *J. Chem. Phys.* **2003**, *119*, 3025.
- (15) Jiang, W.; Hardy, D. J.; Phillips, J. C., Jr.; D. M., A.; Schulten, K.; Roux, B. High-Performance Scalable Molecular Dynamics Simulations of a Polarizable Force Field Based on Classical Drude Oscillators in NAMD. *J. Phys. Chem. Lett.* **2011**, *2*, 87–92.
- (16) Lamoureux, G.; MacKerell, A. D.; Roux, B. A Simple Polarizable Model of Water Based on Classical Drude Oscillators. *J. Chem. Phys.* **2003**, *119*, 5185.
- (17) Lamoureux, G.; Harder, E.; Vorobyov, I. V.; Roux, B.; MacKerell, A. D. A Polarizable Model of Water for Molecular Dynamics Simulations of Biomolecules. *Chem. Phys. Lett.* **2006**, *418*, 245–249.
- (18) Hatcher, E. R.; Guvench, O.; MacKerell, A. D. CHARMM Additive All-Atom Force Field for Acyclic Polyols, Acyclic Carbohydrates, and Inositol. *J. Chem. Theory Comput.* **2009**, *5*, 1315–1327.
- (19) Ponder, J. W.; Wu, C.; Ren, P.; Pande, V. S.; Chodera, J. D.; Schnieders, M. J.; Haque, I.; Mobley, D. L.; Lambrecht, D. S.; DiStasio, R. A., Jr. Current Status of the AMOEBA Polarizable Force Field. *J. Phys. Chem. B* **2010**, *114*, 2549–2564.
- (20) Anisimov, V. M.; Vorobyov, I. V.; Roux, B.; MacKerell, A. D. Polarizable Empirical Force Field for the Primary and Secondary Alcohol Series Based on the Classical Drude Model. *J. Chem. Theory Comput.* **2007**, *3*, 1927–1946.
- (21) Yu, H.; Whitfield, T. W.; Harder, E.; Lamoureux, G.; Vorobyov, I.; Anisimov, V. M.; MacKerell, A. D.; Roux, B. Simulating Monovalent and Divalent Ions in Aqueous Solution Using a Drude Polarizable Force Field. *J. Chem. Theory Comput.* **2010**, *6*, 774–786.
- (22) Diaconis, P.; Efron, B. Computer-Intensive Methods in Statistics. *Sci. Am.* **1983**, *583*, 116.
- (23) Otten, D. E.; Shaffer, P. R.; Geissler, P. L.; Saykally, R. J. Elucidating the Mechanism of Selective Ion Adsorption to the Liquid Water Surface. *Proc. Natl. Acad. Sci. U.S.A.* **2012**, *109*, 701–705.
- (24) Netz, R. R.; Horinek, D. Progress in Modeling of Ion Effects at the Vapor/Water Interface. *Annu. Rev. Phys. Chem.* **2012**, *63*, 401–418.
- (25) Tobias, D. J.; Stern, A. C.; Baer, M. D.; Levin, Y.; Mundy, C. J. Simulation and Theory of Ions at Atmospherically Relevant Aqueous Liquid–Air Interfaces. *Annu. Rev. Phys. Chem.* **2013**, *64*, 339–359.
- (26) Yagasaki, T.; Saito, S.; Ohmine, I. Effects of Nonadditive Interactions on Ion Solvation at the Water/Vapor Interface: A Molecular Dynamics Study. *J. Phys. Chem. A* **2010**, *114*, 12573–12584.
- (27) Stern, A. C.; Baer, M. D.; Mundy, C. J.; Tobias, D. J. Thermodynamics of Iodide Adsorption at the Instantaneous Air–Water Interface. *J. Chem. Phys.* **2013**, *138*, 114709.
- (28) Westh, P.; Rasmussen, E. L.; Koga, Y. Intermolecular Interactions in Ternary Glycerol–Sample–H<sub>2</sub>O: Towards Understanding the Hofmeister Series (V). *J. Solution Chem.* **2010**, *40*, 93–105.
- (29) Rick, S.; Stuart, S. Potentials and Algorithms for Incorporating Polarizability in Computer Simulations. *Rev. Comput. Chem.* **2002**, *18*, 89–146.
- (30) Dang, L. X.; Chang, T.-M. Molecular Mechanism of Ion Binding to the Liquid/Vapor Interface of Water. *J. Phys. Chem. B* **2002**, *106*, 235–238.